International Journal of Thermophysics, Vol. 10, No. 6, 1989

The Thermal Conductivity and Heat Capacity of Gaseous Argon

H. M. Roder,[1] R. A. Perkins,[1] and C. A. Nieto de Castro[2,3]

Received April 3, 1989

This paper presents new absolute measurements of the thermal conductivity and of the thermal diffusivity of gaseous argon obtained with a transient hot-wire instrument. We measured seven isotherms in the supercritical dense gas at temperatures between 157 and 324 K with pressures up to 70 MPa and densities up to 32 mol · L^{-1} and five isotherms in the vapor at temperatures between 103 and 142 K with pressures up to the saturation vapor pressure. The instrument is capable of measuring the thermal conductivity with an accuracy better than 1% and thermal diffusivity with an accuracy better than 5%. Heat capacity results were determined from the simultaneously measured values of thermal conductivity and thermal diffusivity and from the density calculated from measured values of pressure and temperature from an equation of state. The heat capacities presented in this paper, with a nominal accuracy of 5%, prove that heat capacity data can be obtained successfully with the transient hot wire technique over a wide range of fluid states. The technique will be invaluable when applied to fluids which lack specific heat data or an adequate equation of state.

KEY WORDS: argon; dense gas; heat capacity; thermal conductivity; thermal diffusivity; transient hot-wire technique; vapor.

1. INTRODUCTION

Argon is probably the chemical element studied most often. This rare gas is the model system for many theoretical and simulation studies. In particular, many of the efforts toward developing molecular theories of ther-

[1] Thermophysics Division, National Institute of Standards and Technology (formerly National Bureau of Standards), Boulder, Colorado 80303, U.S.A.

[2] Departamento de Quimica, Faculdade de Ciencias, Universidade de Lisboa, 1700 Lisboa, Portugal.

[3] Centro de Quimica Estrutural, Complexo I, IST, 1096 Lisboa Codex, Portugal.

0195-928X/89/1100-1141$06.00/0 © 1989 Plenum Publishing Corporation

modynamic and transport phenomena and reliable computer simulation studies have been based on argon.

It is not surprising that a number of measurements of the thermal conductivity of argon have been reported. However, we prefer measurements made with the transient hot-wire technique over others because the transient hot-wire method, if carefully executed, is expected to have an accuracy better than 1%. Unfortunately, previous transient hot-wire measurements made on argon at this laboratory [1, 2] and at other institutions [3–9] cover only the liquid state [2, 4] and the moderately dense gas [3, 5–9], and only the measurements made at this laboratory extend to pressures of 70 MPa, that is, high densities for the gas. We think that there is a distinct need for accurate measurements in the supercritical dense gas and in the vapor to complement the high-quality data available in the literature for the remainder of the phase diagram.

In a recent correlation developed under the auspices of the Subcommittee on Transport Properties of IUPAC for the thermal conductivity surface of argon [10], the authors report gaps in data coverage, particularly for the thermal conductivity below room temperature, and also that it would be advantageous to extend the range of the thermal conductivity data reported by the transient hot-wire method.

In addition to the thermal conductivity, thermal diffusivity can be measured with transient hot-wire instruments. It has been shown recently that, given an appropriate design of the instrument [11] and a reanalysis of the theory of the method [12], measurements of the thermal diffusivity for all fluids can be made with a reasonable accuracy over wide ranges of density. The heat capacity of fluids can then be obtained from the measurements of thermal conductivity and thermal diffusivity, provided that the density is known [13]. Heat capacity data for argon in the dense gas are rare from direct measurements. At present, the heat capacity of argon is obtained from highly accurate PVT measurements, that is, equations of state, using standard thermodynamic relations, which involve second derivatives. These values can have an estimated error as large as 5%.

We report new extensive measurements of the thermal conductivity and thermal diffusivity of argon at several temperatures, from 103 to 324 K, and pressures up to 70 MPa, covering the supercritical dense gas and the vapor. The thermal conductivity data have an accuracy of better than 1%, while the heat capacity data have an estimated uncertainty of 5%.

2. WORKING EQUATIONS

The transient hot-wire technique is now accepted to be the most accurate method for the measurement of the thermal conductivity of fluids [14]. Its working equation, including the applicable corrections, is well established. The working equation for the temperature rise at the surface of the wire, where $r = r_0$ at time t, is given by

$$\Delta T_{id}(r_0, t) = \frac{q}{4\pi\lambda} \ln \frac{4at}{r_0^2 C} = \frac{q}{4\pi\lambda} \ln\left(\frac{4a}{r_0^2 C}\right) + \frac{q}{4\pi\lambda} \ln(t) \tag{1}$$

In Eq. (1), q is the power input per unit length of wire, λ is the thermal conductivity, $a = \lambda/\rho C_P$ is the thermal diffusivity of the fluid, ρ is its density, C_P is the isobaric heat capacity, and $C = 1.781...$ is the exponential of Euler's constant. We use Eq. (1) and deduce the thermal conductivity from the slope of the straight line of ΔT_{id} versus $\ln(t)$.

To obtain the thermal diffusivity, it was necessary to reanalyze the theory of the method [12]. According to [12] the working equation for the thermal diffusivity is

$$a = \frac{r_0^2 C}{4t'} \exp\left[\frac{4\pi\lambda\, \Delta T_{id}(r_0, t')}{q}\right] \tag{2}$$

The thermal diffusivity is obtained from λ and a value of ΔT_{id} at an arbitrary time t'; $\Delta T_{id}(r_0, t')$ is the intercept of Eq. (1). All sources of departure from the ideal values have been investigated recently for both thermal conductivity and thermal diffusivity [12, 15]. The thermal diffusivity calculated from Eq. (2) must be referred to zero-time conditions, that is, the bath or cell temperature. In summary, the thermal conductivity and the thermal diffusivity evaluated by the data reduction program are related to the reference-state variables and to the zero-time cell variables as follows:

$$\begin{aligned} \lambda &= \lambda(T_r, \rho_r) \\ \rho_r &= \rho(T_r, P_0) \\ a &= a(\rho_0, T_0) = \frac{\lambda(T_0, \rho_0)}{\rho_0 (C_p)_0} \\ \rho_0 &= \rho(T_0, P_0) \\ (C_p)_0 &= C_p(T_0, P_0) \end{aligned} \tag{3}$$

where P_0 is the equilibrium pressure at time $t = 0$.

3. APPARATUS

The apparatus used for the measurements is a general-purpose system [16]. It includes the following elements: two hot wires, a high-pressure cell with wire supports, a Wheatstone bridge, a cryostat, measuring and control circuitry, a sample handling system, and a microcomputer. The hot wires are platinum wires with diameters of 12.7 μm, and the time of measurement extends up to 1 s. The hot wire and a shorter compensating hot wire are arranged in opposing arms of the Wheatstone bridge. The cell containing the core of the apparatus is designed to accommodate pressures from vacuum to 70 MPa at temperatures from 78 to 330 K. The data acquisition system is controlled by a microcomputer and includes two programmable digital voltmeters. We measure the temperature rise in the hot wire at 250 fixed times, 4 ms apart, with a modified Wheatstone bridge, and use linear regression to arrive at the two coefficients of the straight line.

To obtain accurate results for the thermal diffusivity and ultimately for the heat capacity, some changes were made in the original apparatus. These changes improved the measurement of resistance for both bridge and wires, improved the nulling of the bridge prior to applying the power, improved the timing of the experiment, provided some redundancy in the measurement capability, and finally, reduced the noise level in the voltage measurements across the bridge. In particular, since our first measurements of thermal diffusivity [13], a reversing switch driven by the computer was added to the system to improve the resistance measurements in the bridge arms and the zero offset by eliminating any thermal emfs present in the wire and lead connections.

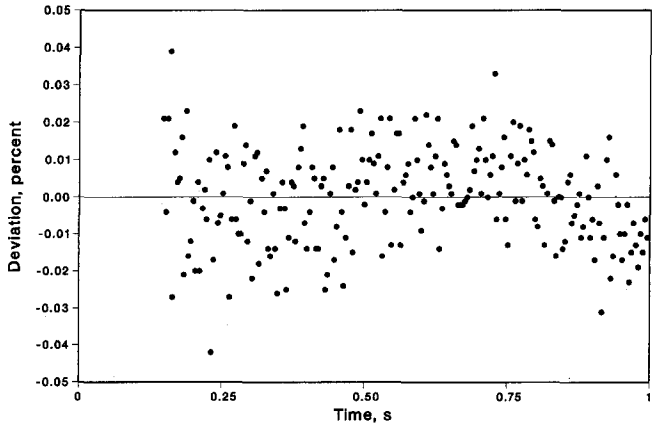

Fig. 1. Deviation plot for a run with argon at $T_r = 221.92$ K and $P_0 = 63.542$ MPa.

The modifications introduced in the equipment were tested in several ways. We compared the data obtained for the thermal conductivity at 300 K with data obtained with the earlier version of the instrument at 300.65 K; the divergence of the results obtained with different power levels decreased from 2 to 0.6%. We found that the deviation of the temperature rises from the linear fit decreased from 0.4 to less than 0.2% when the filter and the operational amplifier were introduced. Finally, we compared the data obtained for the isotherms at 173, 220, and 300 K with data obtained in a different laboratory [3] with a reported accuracy of 0.5%. The maximum deviation between the two sets of data was 1.3% at 173 K and low densities, and the average absolute deviation was 0.5%. This agreement indicates that the data reported here for the thermal conductivity are accurate to better than 1%. Details of the tests can be found in Ref. 11. Figure 1 shows the scatter of the temperature rises for a run at $T = 221.92$ K and $P = 63.542$ MPa; the deviations are not larger than 0.04%.

The argon used for the measurements had a purity in excess of 99.999%. A small diaphragm compressor was used.

4. RESULTS

A total of 1044 data points was measured along seven supercritical isotherms, at nominal temperatures of 157, 173, 203, 223, 274, 302, and 324 K with pressures up to 70 MPa, and along five vapor isotherms, at nominal temperatures of 103, 113, 123, 133, and 142 K. For each pressure, four data points with different powers were taken to verify the absence of convection. These four points were subsequently averaged, and the averages are presented in Tables I and II. The pressure, temperature, and applied power were measured directly, while the density was calculated from an equation of state [17]. A complete tabulation of the data is given in Ref. 18. The results for the thermal conductivity were adjusted at constant density to nominal temperatures by using the preliminary surface fit given in Ref. 18. These adjustments were always less than 0.2%. The error in the thermal conductivity will vary over the entire thermal conductivity surface. Along a normal isotherm the error decreases from low to high densities. If the critical enhancement is appreciable, a curvature in the temperature rise plots is found, probably because of compressibility effects not yet accounted for [15]. In these circumstances the error will increase from low densities to critical density and then decrease at the higher densities. Usually the error in thermal conductivity is described in terms of the regression statistics obtained during the fitting of the straight lines to the data. Statistics for both slope and intercept are recorded in Ref. 18. In our

Table I. The Thermal Conductivity, Thermal Diffusivity, and Heat Capacity of Argon Vapor

Pressure (MPa)	Cell temperature (K)	Thermal conductivity ($W \cdot m^{-1} \cdot K^{-1}$)	Thermal diffusivity ($m^2 \cdot s^{-1}$)	Heat capacity ($J \cdot mol^{-1} \cdot K^{-1}$)
		Nominal temperature, 103 K		
0.193	99.931	0.00703		
0.271	99.932	0.00704		
		Nominal temperature, 113 K		
0.297	109.967	0.00767		
0.458	109.974	0.00776		
0.636	109.982	0.00800	0.393×10^{-6}	24.3
		Nominal temperature, 123 K		
0.343	119.978	0.00833		
0.598	119.976	0.00844	0.596×10^{-6}	20.7
0.852	119.972	0.00877	0.355×10^{-6}	23.9
1.157	119.971	0.00936	0.213×10^{-6}	29.1
		Nominal Temperature, 133 K		
0.286	130.144	0.00906		
0.587	130.137	0.00904		
0.885	130.135	0.00929	0.490×10^{-6}	20.0
1.150	130.128	0.00961	0.332×10^{-6}	22.5
1.400	130.126	0.01002	0.239×10^{-6}	25.4
1.690	130.125	0.01067	0.174×10^{-6}	28.9
2.014	130.131	0.01152	0.103×10^{-6}	40.3
		Nominal temperature, 142 K		
0.446	140.053	0.00960		
0.842	140.045	0.00973	0.617×10^{-6}	19.7
1.159	140.034	0.00998	0.375×10^{-6}	23.3
1.476	140.027	0.01036	0.264×10^{-6}	25.9
1.853	140.021	0.01094	0.179×10^{-6}	30.3
2.244	140.017	0.01182	0.124×10^{-6}	36.6
2.577	140.013	0.01286	0.937×10^{-7}	42.6
2.989	140.018	0.01499	0.637×10^{-7}	56.2

Table II. The Thermal Conductivity, Thermal Diffusivity, and Heat Capacity of Supercritical Argon

Pressure (MPa)	Cell temperature (K)	Thermal conductivity ($W \cdot m^{-1} \cdot K^{-1}$)	Thermal diffusivity ($m^2 \cdot s^{-1}$)	Heat capacity ($J \cdot mol^{-1} \cdot K^{-1}$)
		Nominal temperature, 157 K		
1.225	156.798	0.01068	0.426×10^{-6}	24.4
1.732	156.791	0.01116	0.303×10^{-6}	24.2
2.336	156.789	0.01191	0.200×10^{-6}	27.5
2.650	156.779	0.01235	0.168×10^{-6}	29.2
3.060	156.776	0.01309	0.129×10^{-6}	33.3
3.385	156.761	0.01374	0.108×10^{-6}	36.5
3.825	156.760	0.01490	0.855×10^{-7}	41.8
4.153	156.747	0.01599	0.670×10^{-7}	50.5
4.519	156.739	0.01758	0.521×10^{-7}	62.0
4.927	156.745	0.02006	0.398×10^{-7}	78.3
5.174	156.812	0.02207	0.293×10^{-7}	105.0
5.379	156.812	0.02447	0.223×10^{-7}	137.2
5.550	156.819	0.02719	0.181×10^{-7}	170.1
5.687	156.825	0.03012	0.153×10^{-7}	202.3
5.741	156.815	0.03153	0.129×10^{-7}	240.8
5.817	156.813	0.03359	0.115×10^{-7}	271.4
5.871	156.808	0.03524	0.112×10^{-7}	279.7
5.950	156.816	0.03738	0.109×10^{-7}	284.4
6.011	156.828	0.03888	0.110×10^{-7}	287.6
6.146	156.890	0.04073	0.922×10^{-8}	321.9
6.301	156.908	0.04209	0.100×10^{-7}	282.3
6.496	156.796	0.04279	0.149×10^{-7}	173.5
6.785	156.813	0.04350	0.168×10^{-7}	147.8
7.172	156.817	0.04449	0.203×10^{-7}	118.1
7.664	156.822	0.04572	0.196×10^{-7}	120.5
8.400	156.833	0.04735	0.233×10^{-7}	100.4
9.403	156.843	0.04939	0.278×10^{-7}	84.1
10.405	156.849	0.05121	0.311×10^{-7}	75.8
11.792	156.863	0.05354	0.354×10^{-7}	67.3
13.556	156.874	0.05636	0.402×10^{-7}	60.5
15.713	156.803	0.05949	0.453×10^{-7}	54.8
18.408	156.810	0.06291	0.494×10^{-7}	51.5
20.803	156.811	0.06587	0.536×10^{-7}	48.5
24.081	156.808	0.06931	0.568×10^{-7}	46.9
29.724	156.799	0.07494	0.629×10^{-7}	44.0
35.752	156.805	0.08017	0.671×10^{-7}	42.7
42.578	156.809	0.08587	0.709×10^{-7}	42.0
49.464	156.815	0.09120	0.751×10^{-7}	41.1
57.004	156.815	0.09635	0.818×10^{-7}	38.9
67.589	156.797	0.10328	0.831×10^{-7}	39.9

Table II (*Continued*)

Pressure (MPa)	Cell temperature (K)	Thermal conductivity ($W \cdot m^{-1} \cdot K^{-1}$)	Thermal diffusivity ($m^2 \cdot s^{-1}$)	Heat capacity ($J \cdot mol^{-1} \cdot K^{-1}$)
		Nominal temperature, 173 K		
1.352	171.392	0.01179		
1.933	171.391	0.01220		
2.607	171.396	0.01280		
3.092	171.392	0.01330		
3.573	171.387	0.01394		
4.008	171.410	0.01459		
4.453	171.407	0.01534		
4.799	171.401	0.01601		
5.082	171.397	0.01662		
5.438	171.399	0.01750		
5.745	171.400	0.01835		
5.983	171.397	0.01901		
6.200	171.393	0.01973		
6.473	171.396	0.02074		
6.742	171.386	0.02182		
6.944	171.385	0.02275		
7.214	171.391	0.02390		
7.509	171.395	0.02536		
7.699	171.393	0.02627		
7.868	171.391	0.02722		
8.061	171.391	0.02817		
8.400	171.404	0.03000		
8.652	171.407	0.03121		
8.824	171.327	0.03208		
9.121	171.396	0.03321		
9.418	171.414	0.03442		
9.906	171.421	0.03620		
10.149	171.424	0.03685		
10.504	171.430	0.03790		
10.905	171.434	0.03913		
11.688	172.808	0.04001		
12.323	172.791	0.04151		
12.475	171.420	0.04276		
13.219	172.798	0.04338		
14.155	172.784	0.04494		
16.209	172.795	0.04814		
17.567	172.796	0.05036		
19.820	172.806	0.05342		
21.883	171.423	0.05668		
23.921	171.421	0.05906		
29.429	171.416	0.06510		
35.167	171.422	0.07053		
41.171	171.410	0.07564		
45.408	171.425	0.07896		
53.049	171.415	0.08481		
59.614	171.429	0.08969		
66.115	171.378	0.09376		

Table II (*Continued*)

Pressure (MPa)	Cell temperature (K)	Thermal conductivity ($W \cdot m^{-1} \cdot K^{-1}$)	Thermal diffusivity ($m^2 \cdot s^{-1}$)	Heat capacity ($J \cdot mol^{-1} \cdot K^{-1}$)
		Nominal temperature, 203 K		
2.240	200.576	0.01396	0.408×10^{-6}	23.4
2.870	200.621	0.01435	0.296×10^{-6}	25.4
3.548	200.629	0.01482	0.221×10^{-6}	27.9
4.392	200.630	0.01553	0.170×10^{-6}	29.8
4.876	200.623	0.01597	0.152×10^{-6}	30.3
5.659	200.626	0.01681	0.125×10^{-6}	32.5
6.107	200.627	0.01730	0.114×10^{-6}	33.5
6.929	200.627	0.01834	0.969×10^{-7}	35.6
7.823	200.629	0.01964	0.832×10^{-7}	38.2
8.527	200.624	0.02071	0.714×10^{-7}	42.0
9.031	200.630	0.02156	0.665×10^{-7}	43.6
9.460	200.636	0.02225	0.658×10^{-7}	42.7
10.000	200.637	0.02322	0.592×10^{-7}	46.1
10.484	200.637	0.02409	0.571×10^{-7}	46.6
11.016	200.630	0.02509	0.523×10^{-7}	49.7
11.396	200.622	0.02587	0.513×10^{-7}	50.2
11.861	200.616	0.02676	0.493×10^{-7}	51.4
12.686	200.619	0.02837	0.454×10^{-7}	54.7
13.447	200.621	0.02981	0.447×10^{-7}	54.5
13.990	200.650	0.03082	0.423×10^{-7}	57.1
14.905	200.695	0.03245	0.447×10^{-7}	53.1
15.456	200.726	0.03330	0.437×10^{-7}	54.0
16.124	200.605	0.03462	0.450×10^{-7}	52.4
16.787	200.638	0.03566	0.443×10^{-7}	52.9
17.556	200.628	0.03690	0.454×10^{-7}	51.6
18.738	200.616	0.03858	0.459×10^{-7}	50.8
20.136	200.623	0.04049	0.466×10^{-7}	50.0
21.887	200.604	0.04283	0.493×10^{-7}	47.6
24.539	200.651	0.04582	0.499×10^{-7}	47.3
26.797	200.641	0.04826	0.513×10^{-7}	46.4
30.067	200.641	0.05167	0.525×10^{-7}	46.2
33.467	200.622	0.05490	0.573×10^{-7}	43.2
37.326	200.636	0.05838	0.598×10^{-7}	42.2
41.870	200.649	0.06214	0.625×10^{-7}	41.5
47.446	200.637	0.06641	0.654×10^{-7}	40.8
53.568	200.637	0.07105	0.691×10^{-7}	39.9
58.838	200.641	0.07470	0.717×10^{-7}	39.4
63.758	200.625	0.07800	0.756×10^{-7}	38.2
67.512	200.586	0.08051	0.774×10^{-7}	37.9

Table II (*Continued*)

Pressure (MPa)	Cell temperature (K)	Thermal conductivity ($W \cdot m^{-1} \cdot K^{-1}$)	Thermal diffusivity ($m^2 \cdot s^{-1}$)	Heat capacity ($J \cdot mol^{-1} \cdot K^{-1}$)
		Nominal temperature, 223 K		
1.985	222.822	0.01487	0.594×10^{-6}	22.4
2.699	220.081	0.01521	0.395×10^{-6}	24.3
3.519	220.070	0.01566	0.281×10^{-6}	26.5
4.338	220.065	0.01621	0.223×10^{-6}	27.5
5.035	220.059	0.01672	0.194×10^{-6}	27.6
5.711	220.073	0.01725	0.169×10^{-6}	28.4
6.356	220.073	0.01779	0.160×10^{-6}	27.4
6.951	220.089	0.01837	0.146×10^{-6}	27.9
7.705	220.089	0.01905	0.122×10^{-6}	30.9
8.409	220.061	0.01978	0.109×10^{-6}	32.3
9.126	220.059	0.02056	0.966×10^{-7}	34.4
9.697	220.056	0.02120	0.920×10^{-7}	34.7
10.389	220.061	0.02204	0.862×10^{-7}	35.5
10.807	220.058	0.02255	0.813×10^{-7}	36.8
11.467	220.066	0.02337	0.765×10^{-7}	37.8
11.997	220.055	0.02407	0.726×10^{-7}	38.9
12.581	220.057	0.02483	0.704×10^{-7}	39.2
13.294	220.062	0.02577	0.656×10^{-7}	41.0
13.944	220.059	0.02665	0.631×10^{-7}	41.7
14.597	220.068	0.02750	0.629×10^{-7}	41.1
15.312	220.039	0.02845	0.610×10^{-7}	41.6
16.007	220.068	0.02938	0.592×10^{-7}	42.3
16.582	220.064	0.03012	0.569×10^{-7}	43.5
17.259	220.081	0.03105	0.583×10^{-7}	42.4
18.131	220.075	0.03216	0.566×10^{-7}	42.9
18.780	220.063	0.03298	0.562×10^{-7}	42.9
19.495	220.079	0.03393	0.562×10^{-7}	42.8
20.236	220.071	0.03476	0.548×10^{-7}	43.7
23.128	220.071	0.03821	0.552×10^{-7}	43.1
26.499	220.054	0.04181	0.572×10^{-7}	41.5
29.412	220.068	0.04471	0.585×10^{-7}	40.8
32.406	220.037	0.04734	0.569×10^{-7}	42.3
35.928	220.027	0.05037	0.588×10^{-7}	41.5
39.134	220.030	0.05299	0.614×10^{-7}	40.3
42.488	220.036	0.05563	0.620×10^{-7}	40.6
45.075	219.969	0.05771	0.653×10^{-7}	39.0
48.821	220.032	0.06056	0.681×10^{-7}	38.2
52.785	220.097	0.06342	0.697×10^{-7}	38.0
56.233	220.072	0.06581	0.732×10^{-7}	36.8
59.876	219.273	0.06850	0.737×10^{-7}	37.0
64.383	219.152	0.07158	0.784×10^{-7}	35.6

Table II (*Continued*)

Pressure (MPa)	Cell temperature (K)	Thermal conductivity ($W \cdot m^{-1} \cdot K^{-1}$)	Thermal diffusivity ($m^2 \cdot s^{-1}$)	Heat capacity ($J \cdot mol^{-1} \cdot K^{-1}$)
		Nominal temperature, 274 K		
3.266	270.198	0.01807	0.612×10^{-6}	19.5
4.596	270.198	0.01852	0.393×10^{-6}	21.8
5.954	270.197	0.01919	0.302×10^{-6}	22.5
7.434	270.192	0.01997	0.234×10^{-6}	23.8
9.224	270.190	0.02103	0.182×10^{-6}	25.7
10.598	270.165	0.02186	0.157×10^{-6}	26.7
11.981	270.204	0.02280	0.139×10^{-6}	27.8
13.453	270.201	0.02385	0.126×10^{-6}	28.4
14.875	270.220	0.02489	0.117×10^{-6}	28.8
16.452	270.195	0.02605	0.105×10^{-6}	30.2
18.019	270.200	0.02721	0.944×10^{-7}	32.1
19.477	270.208	0.02838	0.923×10^{-7}	31.7
21.275	270.192	0.02979	0.890×10^{-7}	31.8
22.768	270.215	0.03097	0.853×10^{-7}	32.4
24.342	270.248	0.03223	0.841×10^{-7}	32.3
26.041	270.231	0.03349	0.812×10^{-7}	32.9
27.612	270.195	0.03468	0.783×10^{-7}	33.6
29.060	270.222	0.03572	0.772×10^{-7}	33.7
30.612	270.188	0.03693	0.764×10^{-7}	33.9
31.858	270.222	0.03780	0.771×10^{-7}	33.4
33.310	270.225	0.03887	0.762×10^{-7}	33.6
34.671	270.225	0.03972	0.739×10^{-7}	34.5
36.245	270.221	0.04085	0.734×10^{-7}	34.6
37.918	270.220	0.04186	0.725×10^{-7}	34.9
39.356	270.217	0.04286	0.736×10^{-7}	34.4
41.321	270.216	0.04416	0.737×10^{-7}	34.4
43.136	270.211	0.04541	0.717×10^{-7}	35.4
45.308	270.215	0.04688	0.738×10^{-7}	34.5
47.397	270.219	0.04823	0.743×10^{-7}	34.5
49.264	270.208	0.04936	0.761×10^{-7}	33.7
51.136	270.205	0.05051	0.745×10^{-7}	34.6
53.905	270.216	0.05228	0.755×10^{-7}	34.4
57.467	270.111	0.05437	0.760×10^{-7}	34.5
60.785	270.094	0.05631	0.781×10^{-7}	33.9
64.307	270.105	0.05833	0.802×10^{-7}	33.4
67.468	270.106	0.06012	0.804×10^{-7}	33.6

Table II (*Continued*)

Pressure (MPa)	Cell temperature (K)	Thermal conductivity ($W \cdot m^{-1} \cdot K^{-1}$)	Thermal diffusivity ($m^2 \cdot s^{-1}$)	Heat capacity ($J \cdot mol^{-1} \cdot K^{-1}$)
		Nominal temperature, 302 K		
4.432	298.555	0.01955	0.483×10^{-6}	21.9
6.312	298.562	0.02032	0.340×10^{-6}	22.5
7.851	298.575	0.02103	0.269×10^{-6}	23.6
9.573	298.582	0.02185	0.217×10^{-6}	24.7
10.974	298.576	0.02261	0.195×10^{-6}	24.7
12.340	298.573	0.02345	0.175×10^{-6}	25.4
14.449	298.576	0.02453	0.144×10^{-6}	27.5
16.464	298.567	0.02573	0.133×10^{-6}	27.4
18.551	298.620	0.02698	0.114×10^{-6}	29.8
23.050	298.677	0.02975	0.101×10^{-6}	30.4
25.149	298.664	0.03107	0.900×10^{-7}	32.9
27.467	298.658	0.03260	0.921×10^{-7}	31.3
29.622	298.815	0.03388	0.937×10^{-7}	30.0
31.771	298.814	0.03520	0.941×10^{-7}	29.3
33.875	298.812	0.03651	0.931×10^{-7}	29.2
36.018	298.816	0.03774	0.873×10^{-7}	30.8
38.586	298.836	0.03929	0.864×10^{-7}	30.8
40.776	298.842	0.04055	0.859×10^{-7}	30.8
42.820	298.837	0.04183	0.861×10^{-7}	30.7
44.891	298.832	0.04309	0.852×10^{-7}	31.0
47.308	298.837	0.04440	0.833×10^{-7}	31.7
49.788	298.847	0.04588	0.844×10^{-7}	31.3
52.321	298.994	0.04721	0.845×10^{-7}	31.3
54.745	298.999	0.04862	0.851×10^{-7}	31.2
56.927	298.999	0.04977	0.825×10^{-7}	32.2
58.867	299.001	0.05074	0.850×10^{-7}	31.3
61.171	299.003	0.05206	0.851×10^{-7}	31.5
63.274	298.993	0.05318	0.877×10^{-7}	30.7
65.449	298.991	0.05431	0.873×10^{-7}	31.0
67.301	298.997	0.05520	0.846×10^{-7}	32.0

Table II (*Continued*)

Pressure (MPa)	Cell temperature (K)	Thermal conductivity ($W \cdot m^{-1} \cdot K^{-1}$)	Thermal diffusivity ($m^2 \cdot s^{-1}$)	Heat capacity ($J \cdot mol^{-1} \cdot K^{-1}$)
		Nominal temperature, 324 K		
3.710	321.825	0.02032	0.687×10^{-6}	21.0
5.306	321.863	0.02074	0.451×10^{-6}	22.7
7.537	321.892	0.02172	0.313×10^{-6}	24.0
8.691	321.095	0.02220	0.262×10^{-6}	25.2
11.400	321.093	0.02324	0.196×10^{-6}	26.9
13.592	321.084	0.02441	0.170×10^{-6}	27.2
15.669	321.101	0.02539	0.146×10^{-6}	28.7
17.795	321.089	0.02644	0.129×10^{-6}	29.8
19.831	321.106	0.02756	0.120×10^{-6}	30.0
22.068	321.115	0.02875	0.106×10^{-6}	32.1
24.985	321.114	0.03008	0.105×10^{-6}	30.2
26.686	321.114	0.03133	0.995×10^{-7}	31.4
28.943	321.129	0.03262	0.952×10^{-7}	31.9
31.312	320.815	0.03399	0.945×10^{-7}	31.3
33.677	320.797	0.03526	0.889×10^{-7}	32.6
36.266	320.788	0.03664	0.857×10^{-7}	33.1
38.341	320.776	0.03772	0.862×10^{-7}	32.5
40.694	320.749	0.03918	0.874×10^{-7}	31.9
43.223	320.748	0.04030	0.890×10^{-7}	30.9
45.509	320.765	0.04209	0.894×10^{-7}	31.0
47.771	320.682	0.04271	0.773×10^{-7}	35.2
49.863	320.678	0.04383	0.768×10^{-7}	35.4
52.141	320.680	0.04508	0.784×10^{-7}	34.7
53.909	320.662	0.04601	0.768×10^{-7}	35.4
56.219	320.635	0.04717	0.792×10^{-7}	34.3
58.588	320.730	0.04832	0.790×10^{-7}	34.4
60.566	320.715	0.04921	0.794×10^{-7}	34.3
62.737	320.706	0.05037	0.825×10^{-7}	33.1
65.562	320.734	0.05161	0.772×10^{-7}	35.4
67.919	320.851	0.05293	0.809×10^{-7}	34.1

case, however, a better measure of the error is the dispersion of the results obtained with the four different power levels. This dispersion includes the effect of the statistics above. Considering the variation in power levels, the errors in thermal conductivity are 0.6% for the lowest densities along an isotherm, decreasing to 0.2% for liquid densities. If there is an appreciable critical enhancement the error will increase at intermediate densities, up to 3% for 157 K at the critical density.

Figure 2 displays the variation of the thermal conductivity with density for the different isotherms. The lines in Fig. 2 correspond to the values calculated from the IUPAC correlation [10]. The average absolute deviation between the new measurements and the correlation is 4.9% for the 287 points shown. The deviations are pronounced in the region of the critical enhancement and for all vapor isotherms; they range up to 28%. The nominal deviation at the highest densities is about 2% for most supercritical isotherms. The correlation also shows negative slopes for all vapor isotherms.

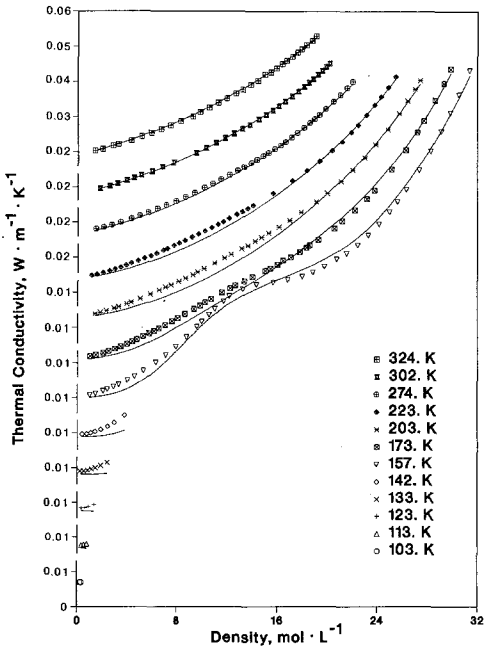

Fig. 2. Thermal conductivity of argon as a function of density for the different isotherms. Each isotherm is displaced by $0.01\ W \cdot m^{-1} \cdot K^{-1}$ from the adjacent isotherms. Lines are from the correlation of Ref. 10.

The values of the measured thermal diffusivity refer to the cell temperature and are displayed in Tables I and II. The heat capacity was obtained from the values of thermal diffusivity, thermal conductivity adjusted to the cell temperature and pressure, and density from the equation of state [17]. Tables I and II show the values of the heat capacity corrected to the nominal temperatures using the equation of state [17]. Errors for the thermal diffusivity exhibit a pattern similar to that of the thermal conductivity. Considering the variation in power levels, the errors in thermal diffusivity are 5% for densities above $1\ \text{mol} \cdot \text{L}^{-1}$ along an isotherm, decreasing to 3% for liquid densities. If there is an appreciable critical enhancement the error will increase at intermediate densities, up to $\pm 10\%$ for 157 K at the critical density.

Figure 3 displays the results obtained for the heat capacity of argon, as a function of density, for the different temperatures in the dense gas and vapor phase. The error in the heat capacity measurements was estimated in two different ways, fully described in Ref. 11. First, the extrapolation of the heat capacity data to zero density has shown an average agreement of

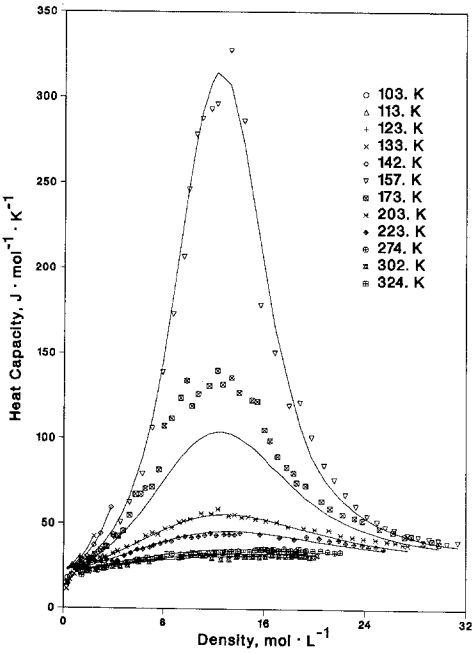

Fig. 3. Heat capacity of argon as a function of density for the different isotherms. Lines are from the equation of state of Ref. 17.

4.4% with the theoretical value of 20.786 $J \cdot mol^{-1} \cdot K^{-1}$. Second, the root-mean-square deviation between the experimental data and the values obtained from the equation of state [17] was about 5%, except for the 173 K isotherm. We trace the larger deviations for the 173 K isotherm, the first isotherm for which we measured the thermal diffusivity, to the absence of the reversing switch. The data for this isotherm were obtained before this device had been introduced in the measuring system. For this reason the data for thermal diffusivity and heat capacity for this isotherm are omitted in Table II. Data in the vapor phase, especially for densities lower than 0.6 $mol \cdot L^{-1}$, also have a large uncertainty in thermal diffusivity due to a low signal-to-noise ratio in the amplifier. These data are also omitted from the tables.

The heat capacities presented in this paper, with a nominal accuracy of 5%, prove that heat capacity data can be obtained successfully with the transient hot-wire technique over a wide range of fluid states. The technique will be invaluable when applied to fluids which lack specific heat data or an adequate equation of state.

5. DATA ANALYSIS

The data presented in Tables I and II cover a large part of the thermal conductivity surface of argon. The data analysis performed on this surface concentrated on two specific aspects, the extraction of the thermal conductivity values at zero density and the evaluation of the critical enhancement. Both of these aspects are discussed in more detail below.

To obtain a value at zero density from the experiment, we must extrapolate the measurements at low density to zero density, usually with a low-order polynomial. For the supercritical isotherms, a linear extrapolation in density was sufficient. However, the vapor isotherms exhibit substantial curvature, as can be seen in Fig. 2. Because of this extreme curvature, we used a graphical extrapolation procedure. We superimposed the vapor isotherms to form a single curve and obtained the curvature with a single fixed spline. The spline was then used to extrapolate each isotherm individually. The results obtained, together with their uncertainty, are shown in Table III. The extrapolation degrades the accuracy of the tabulated values to about 1%, especially in the vapor phase.

We represent our data and all other data obtained with the transient hot-wire method [1, 3, 5-9] with the form of the equation used in the IUPAC correlation [10],

$$\lambda_0 = \sum_{i=1}^{9} a_i T^{(i-4)/3} \tag{4}$$

Table III. The Zero-Density Thermal Conductivity Values for Gaseous Argon

T(K)	$\lambda_0 \pm \sigma$ (mW · m^{-1} · K^{-1})
103.00	6.81 ± 0.07
113.00	7.42 ± 0.07
123.00	8.04 ± 0.08
133.00	8.69 ± 0.09
142.00	9.26 ± 0.09
158.00	10.07 ± 0.10
171.60	10.80 ± 0.07
203.63	12.53 ± 0.09
223.50	13.70 ± 0.11
270.20	16.09 ± 0.17
298.79	17.64 ± 0.19
320.96	18.77 ± 0.12

In Eq. (4), T is expressed in K and λ_0 in mW · m^{-1} · K^{-1}. Using all 29 points the coefficients were found to be

$$a_1 = 4.82935 \times 10^{+4}$$
$$a_2 = -7.20940 \times 10^{+4}$$
$$a_3 = 4.93535 \times 10^{+4}$$
$$a_4 = -1.97168 \times 10^{+4}$$
$$a_5 = 4.92040 \times 10^{+3}$$
$$a_6 = -7.74316 \times 10^{+2}$$
$$a_7 = 7.45021 \times 10^{+1}$$
$$a_8 = -3.97878$$
$$a_9 = 9.00908 \times 10^{-2}$$

and the standard deviation of the fit was 0.06 mW · m^{-1} · K^{-1}. This standard deviation is equivalent to a deviation of 0.9% at 100 K and 0.3% at 425 K.

Figure 4 shows the deviations from Eq. (4) of all data points included in the fit; all deviations are less than 1%. Also in Fig. 4, in the curve labeled 1, are the deviations between Eq. (4) and the IUPAC correlation [10]. The range of this correlation is 90 to 500 K, and it is constrained to the dilute gas values of Kestin et al. [19], which were established using an extended law of corresponding states. There are large departures for tem-

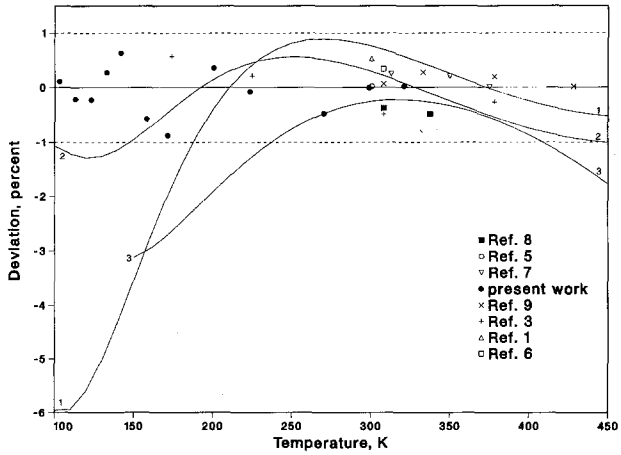

Fig. 4. Devations between Eq. (4) and the experimental data points. The lines describe the correlations: (1) Kestin et al. [19]; (2) Rabinovich et al. [23]; (3) Trappeniers [24].

peratures lower than 180 K, for example, 6% at 100 K, while the agreement is within 1% at the higher temperatures. The excellent agreement obtained with Refs. 10 and 19 for temperatures greater than 180 K leads us to examine the much larger deviations at the low temperatures. Kestin et al. [19] did not select any primary data for either viscosity or thermal conductivity of argon, krypton, or xenon[4] at temperatures below 300 K. The authors did consider the viscosity data obtained with the capillary tube method by Clarke and Smith [20] as secondary data. These viscosity values [20] are 2% larger at 114 K than the correlated values of Kestin et al. for all three noble gases.

The low-temperature viscosity data of Johnston et al. [21, 22], not considered in Ref. 19, agree well with the present thermal conductivity values. Eucken factors of 1.013 were calculated at 103 and 113 K; this implies an agreement of 1.3% between our thermal conductivity values and the viscosities of Ref. 22. Johnston et al. obtained their values with an oscillating disk viscometer, and their values are about 3% higher than those reported by Clarke and Smith [20] at 114 K. The differences between the two sets of viscosity data decrease to less than 1% for temperatures between 130 and 300 K. Rabinovich et al. [23] also noted the discrepancies between these two sets of viscosity data. By considering internal consistency with thermal conductivity data, these authors preferred the viscosity data of Johnston et al. [21, 22]. Their tables for the thermal

[4] Argon at 100 K corresponds to krypton at 139 K and xenon at 192 K.

conductivity of dilute gaseous argon agree with our data to within 1.3% at the lowest temperature and are shown in Fig. 4 as the curve labeled 2.

Finally, we show in Fig. 4, in the curve labeled 3, the deviations between Eq. (4) and the equation proposed by Trappeniers [24]. Trappeniers correlated his measurements obtained with the parallel-plate apparatus for temperatures above the critical point. Deviations between his representation and Eq. (4) are as large as -2% at a temperature of 200 K and increase to -3% at a temperature of 150 K.

We conclude that the correlations given in Refs. 10, 19, and 24 for the zero-density thermal conductivity of argon are in error for temperatures below 180 K. We suggest that Eq. (4), which has a maximum uncertainty of 1% at a 99% confidence level, is the best empirical representation of the zero-density thermal conductivity of argon over the temperature range from 100 to 450 K.

The second part of the data analysis concerns the evaluation of the critical enhancement. The dependence of the thermal conductivity on temperature and density in the supercritical region is usually expressed as

$$\lambda(\rho, T) = \lambda_0(T) + \Delta\lambda(\rho, T) + \Delta\lambda_0(\rho, T) \tag{5}$$

where the first term is the zero-density gas thermal conductivity, $\Delta\lambda$ is the excess thermal conductivity over the dilute-gas value, and $\Delta\lambda_c$ is the critical enhancement. The first two terms on the right-hand side of Eq. (5) are collectively referred to as the "background" thermal conductivity. Since large systematic deviations are evident between our results and the most recent correlation of the thermal conductivity surface of argon [10], we could not use this surface to evaluate the critical enhancement. Instead we used the preliminary surface fit given in Ref. 18, which has an average absolute deviation of 1.15% for the 287 points presented in Tables I and II. The maximum deviation is 8.9% at 142 K in the vapor phase near saturation pressure. The surface fit of Ref. 18 is based on experimental data for argon measured with the present instrument: included are the seven supercritical isotherms, three of the five vapor isotherms, 113, 123, and 142 K, and the three liquid-phase isotherms, 111, 125, and 140 K, from Ref. 2. The zero-density thermal conductivity is given by Eq. (4). The remainder of the surface is described in more detail below.

The expression for the excess thermal conductivity was previously used for methane [25] and it is

$$\Delta\lambda = \alpha(T)\,\rho + \beta(T)\,\rho^{n(T)} \tag{6}$$

with $\Delta\lambda$ expressed in $\mathrm{W \cdot m^{-1} \cdot K^{-1}}$, ρ in $\mathrm{mol \cdot L^{-1}}$, and T in K. The parameters α, β, and n are functions of the temperature. The α was deter-

mined from the slopes of the isotherms at low density and was found to vary linearly with temperature:

$$\alpha = \alpha_1 + \alpha_2 T \qquad \text{with } \alpha_1 = 5.2 \times 10^{-4} \qquad \text{and } \alpha_2 = 1.6 \times 10^{-6} \tag{7}$$

The coefficient n can be represented by a low-order polynomial in temperature,

$$n = n_1 + n_2 T + n_3 T^2 \tag{8}$$

while β, varying through an order of magnitude, is better expressed by fitting the logarithm of β,

$$\ln \beta = \beta_1 + \beta_2 T + \beta_3 T^2 + \beta_4 T^3 \tag{9}$$

The coefficients n_i and β_i were determined in a single surface fit:

$$n_1 = 3.391792$$
$$n_2 = -3.138159 \times 10^{-3}$$
$$n_3 = 5.773095 \times 10^{-6}$$
$$\beta_1 = -1.425607 \times 10^{+1}$$
$$\beta_2 = 1.007190 \times 10^{-2}$$
$$\beta_3 = -1.906250 \times 10^{-5}$$
$$\beta_4 = -2.651697 \times 10^{-9}$$

An approximation to the critical enhancement $\Delta\lambda_c$ can now be obtained from Eq. (5) by subtracting values from Eqs. (4) and (6) from the experimental thermal conductivities. The remainders are plotted in Fig. 5 for nominal temperatures. All isotherms reported here are outside the critical region proper as defined by Sengers et al. [26], and therefore, there was no need to use a scaled equation of state. For argon, $T_c = 150.86$ K and $\rho_c = 13.41$ mol $\cdot$ L^{-1} [17], and the boundaries of the critical region proper are $146.33 \leqslant T \leqslant 155.4$ K and $10.06 \leqslant \rho \leqslant 16.76$ mol $\cdot$ L^{-1}.

To represent the critical enhancement we have followed a procedure similar to that used for methane [25] and oxygen [27], because the behavior of argon was similar to that of these gases. The critical enhancement extends to quite high temperatures, $>2T_c$, confirming the data previously reported [1]. Also, the critical enhancement is centered on a density ρ_{center}, which is different from the critical density ρ_c and slightly temperature dependent. Finally, the data proved to be slightly asymmetric

about ρ_{center}. The expression used to represent the critical enhancement is given by

$$\Delta\lambda_c(\rho, T) = \text{AMPL}\, e^{-x^2} \tag{10}$$

with

$$\text{AMPL} = \frac{C_1}{T + C_2} + C_3 + C_4 T \tag{11}$$

$$\rho_{\text{center}} = \rho_c + C_5(T - T_c)^{1.5} \tag{12}$$

and

$$x = C_6(\rho - \rho_{\text{center}}) \qquad \text{for } \rho \leqslant \rho_{\text{center}} \tag{13}$$

or

$$x = C_7(\rho - \rho_{\text{center}}) \qquad \text{for } \rho \geqslant \rho_{\text{center}} \tag{14}$$

The coefficients C_i, as determined by the surface fit, are given by

$$C_1 = 1.115727 \times 10^{-1}$$

$$C_2 = -1.49 \times 10^{+2}$$

$$C_3 = 4.059586 \times 10^{-3}$$

$$C_4 = -1.280545 \times 10^{-5}$$

$$C_5 = -9.918980 \times 10^{-4}$$

$$C_6 = -1.5230 \times 10^{-1}$$

$$C_7 = 1.6494 \times 10^{-1}$$

again with T in K, ρ in $\text{mol} \cdot \text{L}^{-1}$, and $\Delta\lambda_c$ in $\text{W} \cdot \text{m}^{-1} \cdot \text{K}^{-1}$.

Values calculated from Eqs. (10) to (14) are shown as continuous lines for the isotherms 157 to 324 K in Fig. 5.

Values of $\Delta\lambda_c(\rho_c, T)$ can now be obtained from Eq. (14), using $\rho = \rho_c$. The variation of $\Delta\lambda_c(\rho_c, T)$ with $\Delta T^* = [(T - T_c)/T_c]$ follows a power law of the type

$$\Delta\lambda_c(\rho_c, T) = A(\Delta T^*)^{-\phi} \tag{15}$$

for temperatures very close to the critical point. For argon, Trappeniers [24] proposed an asymptotic value ϕ_∞ of 0.57, and a value $\phi_{\text{emc}} = 0.635 \pm 0.015$ based on a variation of the extended-mode-coupling theory.

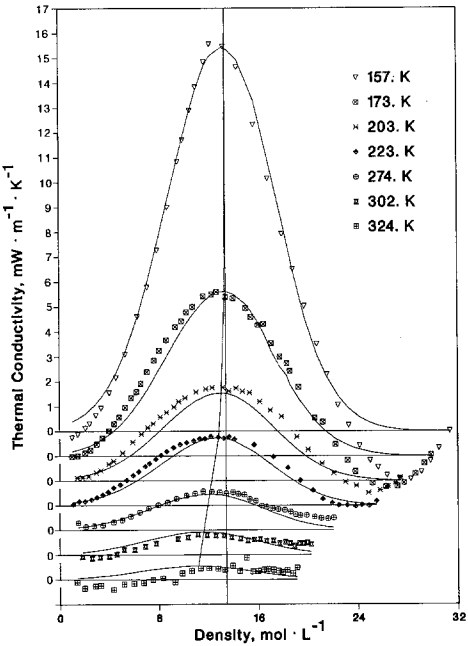

Fig. 5. The critical enhancement function $\Delta\lambda_c(\rho, T)$. The lines are given by Eqs. (10) to (14). Isotherms are separated by $0.001\ W \cdot m^{-1} \cdot K^{-1}$. The curve to the left of ρ_c is the locus of values of ρ_{center}.

Figure 6 shows the data of Trappeniers [24], Bailey and Kellner [28, 29], Ikenberry and Rice [30], and Nieto de Castro and Roder [1], along with the present data, for $\Delta\lambda_c(\rho_c, T)$ as a function of ΔT^*. There are systematic deviations among the different sets of data, most likely caused by differences in the "background" thermal conductivity. The value of the critical enhancement is quite sensitive to the background, and the way in which the background is determined often depends on the amount of data available and its range in both density and temperature. Ideally, all of the data given in Fig. 6 should have been reduced using a single thermal conductivity surface.

The critical enhancement in argon extends to temperatures of $\Delta T^* = 1.15$. At the highest temperature, 324 K, the enhancement is about $0.5\ mW \cdot m^{-1} \cdot K^{-1}$ or 1.7% of the total conductivity. If our 324 K isotherm were taken unchanged as an approximation for the background of the other isotherms, an uncertainty of about 2% would be introduced into the derived critical region data.

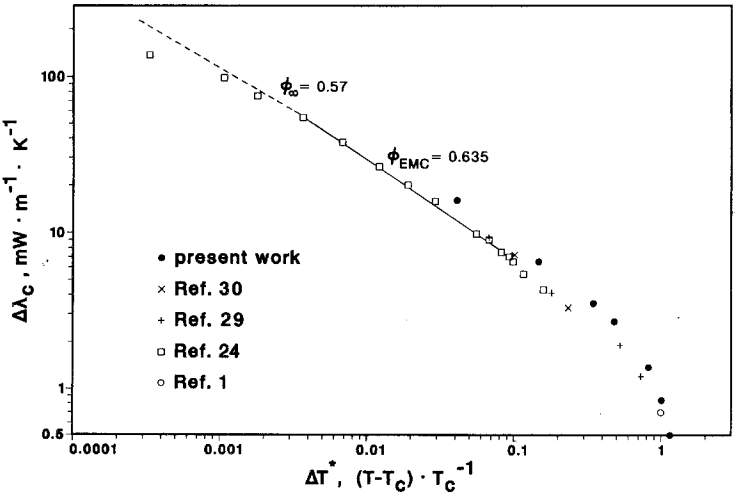

Fig. 6. The variation of $\Delta\lambda_c(\rho_c, T)$ with respect to ΔT^*.

6. CONCLUSIONS

The correlations given in Refs. 10, 19, and 24 for the zero-density thermal conductivity of argon are in error for temperatures below 180 K. We suggest that Eq. (4), which has a maximum uncertainty of 1% at a 99% confidence level, is the best empirical representation of the zero-density thermal conductivity of argon over the temperature range from 100 to 450 K.

We recommend that a new effort to correlate the thermal conductivity surface of argon be undertaken, since, in our opinion, neither the IUPAC correlation [10] nor our preliminary surface [18] is an adequate representation.

ACKNOWLEDGMENTS

We thank Professor W. A. Wakeham, Imperial College, London, for many discussions on the development of the corrections to the transient hot-wire theory to obtain the thermal diffusivity and Drs. B. A. Younglove, R. D. McCarty, and J. W. Magee, National Institute of Standards and Technology, for many suggestions regarding the use of the IUPAC correlation and the accuracy of the heat capacity data. One of the authors (C.A.N.C.) thanks the Faculty of Sciences of the University of Lisbon for a leave of absence and the Thermophysics Division of the National Institute of Standards and Technology for having invited him as a Guest Scientist.

REFERENCES

1. C. A. Nieto de Castro and H. M. Roder, *J. Res. Natl. Bur. Stand. (U.S.)* **86**:293 (1981).
2. H. M. Roder, C. A. Nieto de Castro, and U. V. Mardolcar, *Int. J. Thermophys.* **8**:521 (1987).
3. U. V. Mardolcar, C. A. Nieto de Castro, and W. A. Wakeham, *Int. J. Thermophys.* 7:259 (1986).
4. J. C. G. Calado, U. V. Mardolcar, C. A. Nieto de Castro, H. M. Roder, and W. A. Wakeham, *Physica* **143A**:314 (1987).
5. J. Kestin, R. Paul, A. A. Clifford, and W. A. Wakeham, *Physica* **100A**:349 (1980).
6. M. J. Assael, M. Dix, A. Lucas, and W. A. Wakeham, *J. Chem. Soc. Faraday Trans.* **77**:439 (1981).
7. A. A. Clifford, P. Gray, A. I. Johns, A. C. Scotts, and J. T. R. Watson, *J. Chem. Soc. Faraday Trans.* **77**:2679 (1981).
8. E. N. Haran. G. C. Maitland, M. Mustafa, and W. A. Wakeham, *Ber. Bunsenges. Phys. Chem.* **87**:657 (1983).
9. J. Millat, M. Mustafa, M. Ross, W. A. Wakeham, and M. Zalaf, *Physica* **145A**:461 (1987).
10. B. A. Younglove and H. J. Hanley, *J. Phys. Chem. Ref. Data* **15**:1323 (1986).
11. H. M. Roder and C. A. Nieto de Castro, in *Thermal Conductivity 20*, D. P. H. Hasselman and J. R. Thomas, Jr., eds., (Plenum Publishing Co., New York, 1989), p. 173.
12. C. A. Nieto de Castro, B. Taxis, H. M. Roder, and W. A. Wakeham, *Int. J. Thermophys.* **9**:293 (1988).
13. H. M. Roder and C. A. Nieto de Castro, *Cryogenics* **27**:312 (1987).
14. C. A. Nieto de Castro, *JSME Int. J.* **31**:387 (1988).
15. J. M. N. A. Fareleira and C. A. Nieto de Castro, *High Temp.-High Press*, 1989, in press.
16. H. M. Roder, *J. Res. Natl. Bur. Stand. (U.S.)* **86**:457 (1981).
17. B. A. Younglove, *J. Phys. Chem. Ref. Data* **11**:Suppl. 1 (1982).
18. H. M. Roder, R. A. Perkins, and C. A. Nieto de Castro, National Institute of Standards and Technology NISTIR 89-3902 (Oct. 1988).
19. J. Kestin, K. Knierim, E. A. Mason, B. Najafi, S. T. Ro, and M. Waldman, *J. Phys. Chem. Ref. Data* **13**:229 (1984).
20. A. G. Clarke and E. B. Smith, *J. Chem. Phys.* **48**:3988 (1986).
21. H. L. Johnston and K. E. McCloskey, *J. Phys. Chem.* **44**:1038 (1940).
22. H. L. Johnston and E. R. Grilly, *J. Phys. Chem.* **46**:948 (1942).
23. V. A. Rabinovich, A. A. Vasserman, V. I. Nedostup, and L. S. Veksler, in *Thermophysical Properties of Neon, Argon, Krypton and Xenon*, T. B. Selover, Jr., ed. (Hemisphere, Washinton, D.C., 1988), p. 203.
24. N. J. Trappeniers, in *Proc. 8th Symp. Thermophys. Prop.* J. V. Sengers, ed. (ASME, New York, 1982), p. 232.
25. H. M. Roder, *Int. J. Thermophys.* **6**:119 (1985).
26. J. V. Sengers and J. M. H. Levelt Sengers, in *Progress in Liquid Physics*, C. A. Croxton, ed. (John Wiley & Sons, New York, 1978), p. 103.
27. H. M. Roder, *J. Res. Natl. Bur. Stand. (U.S.)* **87**:279 (1982).
28. B. J. Bailey and K. Kellner, *Br. J. Appl. Phys.* **18**:1645 (1968).
29. B. J. Bailey and K. Kellner, *Physica* **31**:444 (1968).
30. L. D. Ikenberry and S. A. Rice, *J. Chem. Phys.* **39**:156 (1963).